

INFORMAL SEGREGATED ALGORITHM AND ITS APPLICATION FOR
SIMULATION OF FLUID FLOWS IN MICRO LIQUID-PROPELLANT
ENGINE

S.I. Martynenko, L.S. Yanovskiy

*Central Institute of Aviation Motors n.a. Baranov (CIAM)
Aviamotornya Str, 2, 111116 Moscow, Russia
Email: martyn_s@mail.ru, web page: http://www.ciam.ru*

Key words: Navier-Stokes equations, numerical methods, structured grids.

Abstract. A new algorithm for solving Navier-Stokes equations in primitive variables on structured grids is proposed. Auxiliary problem is offered to simplify computation of pressure. Part of pressure is computed using mass conservation equations. Residuary part of pressure can be computed by standard methods. The algorithm is especially effective for simulation of directed flows. Description of the informal segregated algorithm (including the auxiliary problem formulation) and application for solving benchmark and industrial problems are given in the paper.

1. INTRODUCTION

Steady two-dimensional Navier-Stokes equations for the incompressible fluid are written as:

1) continuity equation

$$\frac{\partial u}{\partial x} + \frac{\partial v}{\partial y} = 0, \quad (1)$$

2) X-momentum

$$\frac{\partial(u^2)}{\partial x} + \frac{\partial(uv)}{\partial y} = -\frac{\partial p}{\partial x} + \frac{1}{\text{Re}} \left(\frac{\partial^2 u}{\partial x^2} + \frac{\partial^2 u}{\partial y^2} \right), \quad (2)$$

3) Y-momentum

$$\frac{\partial(uv)}{\partial x} + \frac{\partial(v^2)}{\partial y} = -\frac{\partial p}{\partial y} + \frac{1}{\text{Re}} \left(\frac{\partial^2 v}{\partial x^2} + \frac{\partial^2 v}{\partial y^2} \right), \quad (3)$$

Finite-differenced Eqs. (1)-(3) can be written in the following matrix form

$$\begin{pmatrix} a_{11} & a_{12} & a_{13} \\ a_{21} & a_{22} & a_{23} \\ a_{31} & a_{32} & 0 \end{pmatrix} \begin{pmatrix} u \\ v \\ p \end{pmatrix} = \begin{pmatrix} b_1 \\ b_2 \\ b_3 \end{pmatrix}. \quad (4)$$

It is clear that the set (4) cannot be solved by standard methods because of absence of pressure in the continuity equation (1). Now SIMPLE method¹ is prevailing algorithm for solving the Navier-Stokes equations. Main defect of the approach consists of

artificial boundary conditions for pressure-correction equation. Note that some algorithms (for example, artificial compressibility method²) can solve the Navier-Stokes equations without artificial boundary conditions for pressure. Now coupled solvers are proposed and developed, however similar methods are difficult to apply to compressible flows.

Let us consider the fluid flows between parallel plates. The Navier-Stokes equations in boundary layer approximation can be written as:

1) continuity equation

$$\frac{\partial u}{\partial x} + \frac{\partial \vartheta}{\partial y} = 0 \quad , \quad (5)$$

2) X-momentum

$$\frac{\partial(u^2)}{\partial x} + \frac{\partial(u\vartheta)}{\partial y} = -\frac{dp}{dx} + \frac{1}{\text{Re}} \left(\frac{\partial^2 u}{\partial x^2} + \frac{\partial^2 u}{\partial y^2} \right) \quad , \quad (6)$$

3) mass conservation equation

$$\int_0^1 u(0, y) dy = \int_0^1 u(x, y) dy \quad . \quad (7)$$

Very effective numerical methods for solving Eqs. (5)-(7) have been proposed and developed³.

Informal segregated algorithm uses the effective numerical methods for solving the Navier-Stokes equations (1)-(3). For the given purpose, an auxiliary problem is formulated. Solution of the auxiliary problem is close to solution of the Navier-Stokes equations. However computational costs of the auxiliary problem is much less than the cost of Navier-Stokes equations. Informal segregated algorithm is organized in “predictor” (auxiliary problem) and “corrector” (the Navier-Stokes equations) manner. Proposed solver can be used for simulation of 2D and 3D (un)steady (in)compressible flows in primitive variables. Single limitation is requirement of structuredness of the computational grids.

2. DESCRIPTION OF INFORMAL SEGREGATED ALGORITHM

For reason of simplicity, we consider flow in driven cavity (Fig. 1). First, integration of the continuity equation (1) over the control volumes V_1 and V_2 gives

$$\int_0^1 u(x, y) dy = 0 \quad , \quad (8)$$

$$\int_0^1 \vartheta(x, y) dx = 0 \quad . \quad (9)$$

Second, the pressure can be represented as

$$p(x, y) = p^x(x) + p^y(y) + p^{xy}(x, y) \quad . \quad (10)$$

Note that

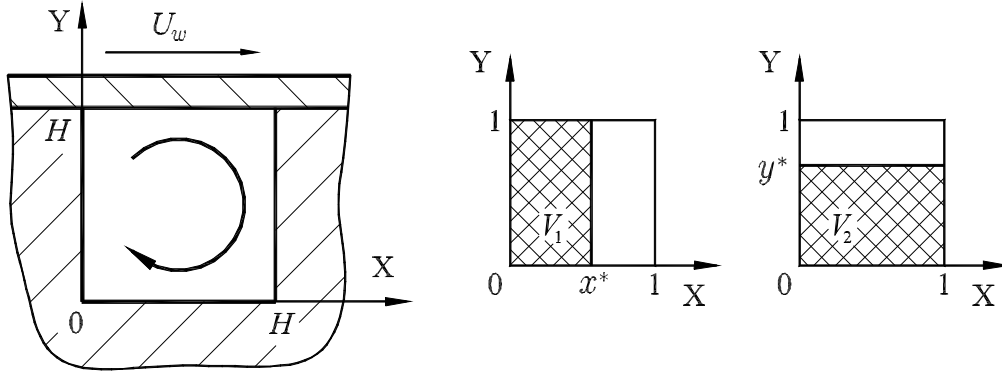


Figure 1. Driven cavity and control volumes V_1 and V_2

$$\frac{\partial p}{\partial x} = \frac{dp^x}{dx} + \frac{\partial p^{xy}}{\partial x} \quad \text{and} \quad \frac{\partial p}{\partial y} = \frac{dp^y}{dy} + \frac{\partial p^{xy}}{\partial y}.$$

Taking into account Eqs.(8)-(10), we obtain the following auxiliary problem:

1) X-momentum and mass flow conservation equation

$$\left\{ \begin{array}{l} \frac{\partial(u^2)}{\partial x} + \frac{\partial(u\vartheta)}{\partial y} = -\frac{dp^x}{dx} - \left[\frac{\partial p^{xy}}{\partial x} \right] + \frac{1}{\text{Re}} \left(\frac{\partial^2 u}{\partial x^2} + \frac{\partial^2 u}{\partial y^2} \right), \\ \int_0^1 u(x, y) dy = 0 \end{array} \right. , \quad (11)$$

2) Y-momentum and mass flow conservation equation

$$\left\{ \begin{array}{l} \frac{\partial(u\vartheta)}{\partial x} + \frac{\partial(\vartheta^2)}{\partial y} = -\frac{dp^y}{dy} - \left[\frac{\partial p^{xy}}{\partial y} \right] + \frac{1}{\text{Re}} \left(\frac{\partial^2 \vartheta}{\partial x^2} + \frac{\partial^2 \vartheta}{\partial y^2} \right), \\ \int_0^1 \vartheta(x, y) dx = 0 \end{array} \right. , \quad (12)$$

where square brackets mean that the pressure gradients are fixed (i.e. its values are taken from previous iterations). The auxiliary problem (11) and (12) can be solved by numerical methods proposed for solution of the Navier-Stokes equations in boundary layer approximation (5)-(7).

Accounting representation (10), the Navier-Stokes equations (1)-(3) (“corrector”) take the form:

1) continuity equation

$$\frac{\partial u}{\partial x} + \frac{\partial \vartheta}{\partial y} = 0 ,$$

2) X-momentum

$$\frac{\partial(u^2)}{\partial x} + \frac{\partial(u\vartheta)}{\partial y} = -\frac{\partial p}{\partial x} - \left[\frac{dp^x}{dx} \right] + \frac{1}{\text{Re}} \left(\frac{\partial^2 u}{\partial x^2} + \frac{\partial^2 u}{\partial y^2} \right) ,$$

3) Y-momentum

$$\frac{\partial(uv)}{\partial x} + \frac{\partial(v^2)}{\partial y} = -\frac{\partial p}{\partial y} - \left[\frac{dp^y}{dy} \right] + \frac{1}{\text{Re}} \left(\frac{\partial^2 v}{\partial x^2} + \frac{\partial^2 v}{\partial y^2} \right),$$

In order to illustrate influence of the auxiliary problem (11) and (12) on convergence rate, we solve the Navier-Stokes equations starting iterand zero: $u = 0, v = 0, p = 0$. In this case classical segregated algorithm (CSA) starts from the problem:

$$\frac{\partial(u^2)}{\partial x} = \frac{1}{\text{Re}} \left(\frac{\partial^2 u}{\partial x^2} + \frac{\partial^2 u}{\partial y^2} \right).$$

According to (12), informal segregated algorithm (ISA) starts from the problem:

$$\begin{cases} \frac{\partial(u^2)}{\partial x} = -\frac{dp^x}{dx} + \frac{1}{\text{Re}} \left(\frac{\partial^2 u}{\partial x^2} + \frac{\partial^2 u}{\partial y^2} \right) \\ \int_0^1 u(x, y) dy = 0 \end{cases}$$

Fig. 2 represents results of the problem solutions (Re=100, staggered grid 101x101). It is easy to see that coupled computation of the velocity component u and “part” of pressure p^x gives more accurate approximation to the solution of the Navier-Stokes equations (1)-(3).

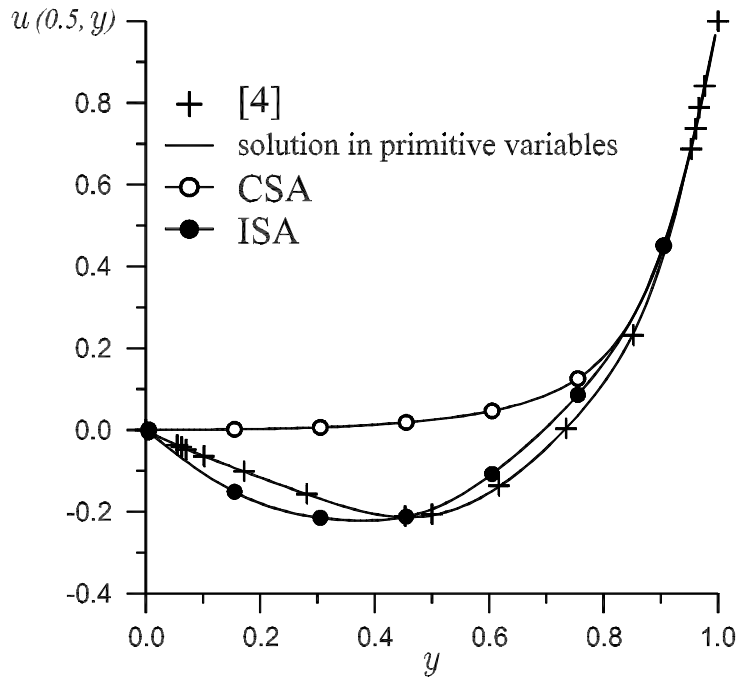


Figure 2. Distribution of u –velocity in middle vertical section of the cavity (Re=100)

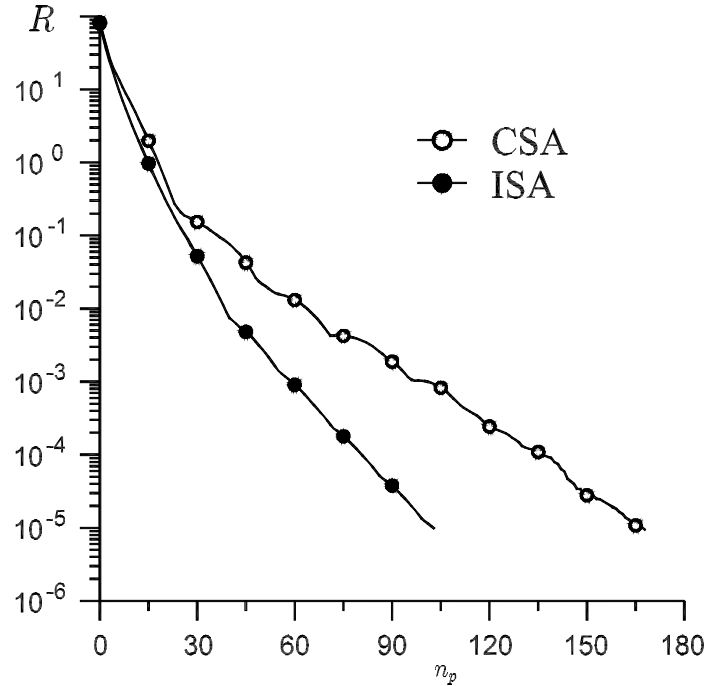


Figure 3. Convergence of CSA and ISA for flow in driven cavity (Re=100)

Convergence of CSA and ISA can be illustrated by maximum error of the finite-differenced continuity equation (1)

$$R = \max_{ij} \left| \frac{u_{i+1j} - u_{ij}}{h} + \frac{v_{ij+1} - v_{ij}}{h} \right|,$$

where h is grid spacing. Fig. 3 shows that coupled computation of the velocity components and “part” of pressure ($p^x + p^y$) results in reduction of pressure iterations n_p . Method of artificial compressibility is used for computation of p^y in (10).

Note that flow in the driven cavity has no preferred direction. As a result, ISA shows the least convergence acceleration as compared with CSA for similar problems.

3. FLOW OVER A BACKWARD-FACING STEP

Fig. 4 represents the problem geometry. Simulation of the flow over a backward-facing step is performed at $Re = 800$ on staggered computational grid 101×1501 . Comparison with data of other authors is given in table 1. Numerical experiments show that application of ISA leads to reduction of execution time in 400 times as compared with CSA. Fig. 5 shows isobars and explains the convergence acceleration. Except for small subdomain, pressure is changed almost linearly. In this case, component p^x in (10) is dominant and computational efforts for solving the Navier-Stokes equations tend to the efforts for boundary layer approximation. Therefore ISA results in impressive convergence acceleration for problems with directed fluid flows.

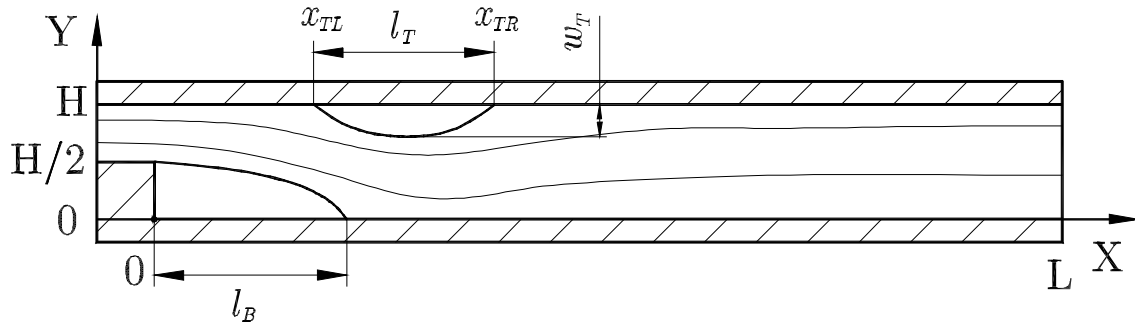


Figure 4. Problem geometry and vortices location

Author	l_B	l_T	ω_T	x_{TL}	x_{TR}	nodes
Barton I.E. ⁵	6.0150	5.6600	-	4.8200	10.4800	
Gartling D. ⁶	6.1000	5.6300	-	4.8500	10.4800	129681
Gresho P.M. ⁷	6.0820	5.6260	-	4.8388	10.4648	245760
Gresho P.M. ⁷	6.1000	5.6300	-	4.8600	10.4900	≥ 8000
Keslar J. ⁸	6.0964	5.6251	-	4.8534	10.4785	3737
present	6.1000	5.6300	0.28	4.8400	10.4700	151601

Table 1. Comparison of results

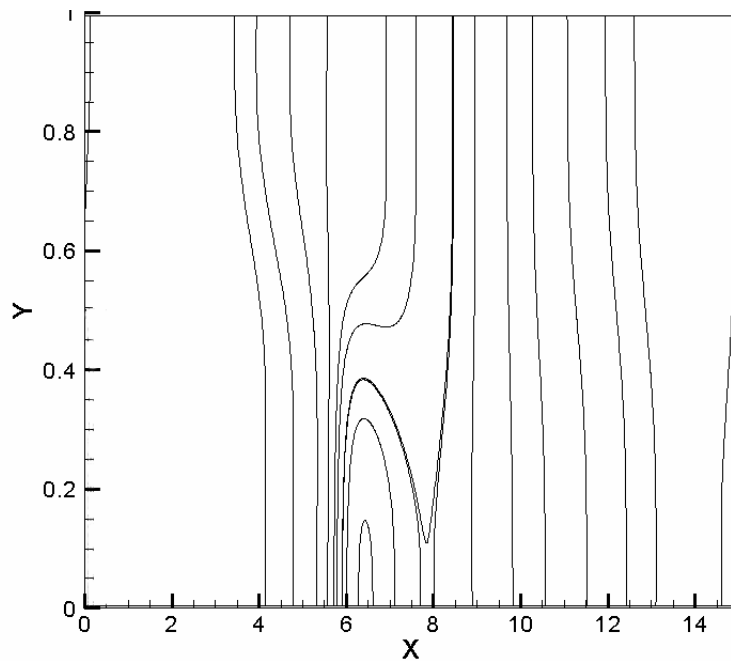


Figure 5. Isobars at flow in over a backward-facing step is performed (Re=800)

4. FLOW IN CATALYST OF MICRO LIQUID-PROPELLANT ENGINE

Efficiency of micro liquid-propellant engine depends strongly on medium decomposition on catalyst. Geometry of typical catalyst is shown on Fig. 6. It is very difficult to use artificial boundary conditions for pressure in similar problems. Staggered grid 385x3150 is used for simulation fluid flow in the catalyst. Figures 7 and 8 represent isolines of stream function and isobars near first column of the catalyst needles. Vortex formation near last column of the catalyst needles is shown on Fig. 9.

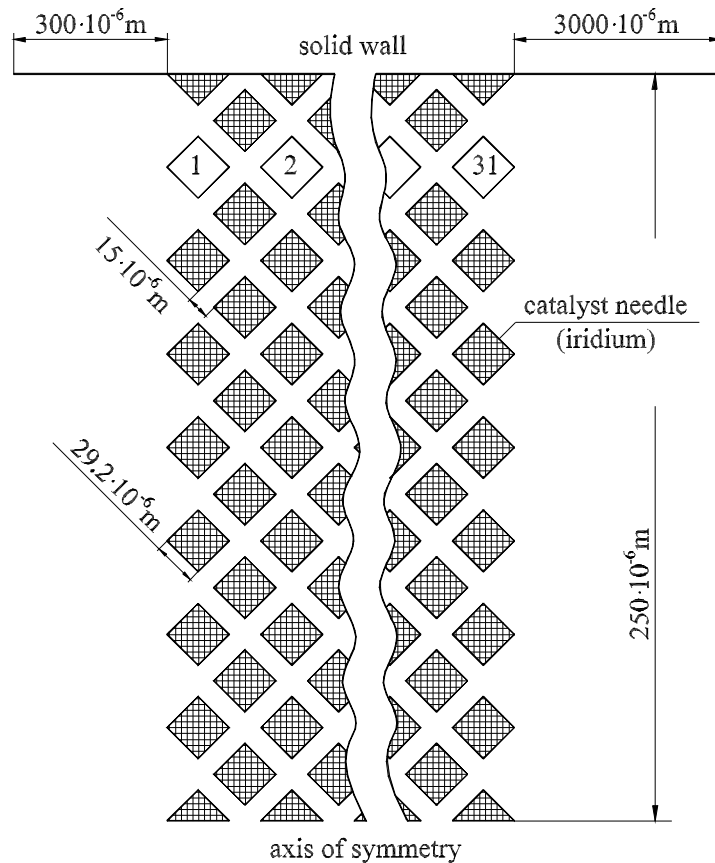


Figure 6. The catalyst geometry

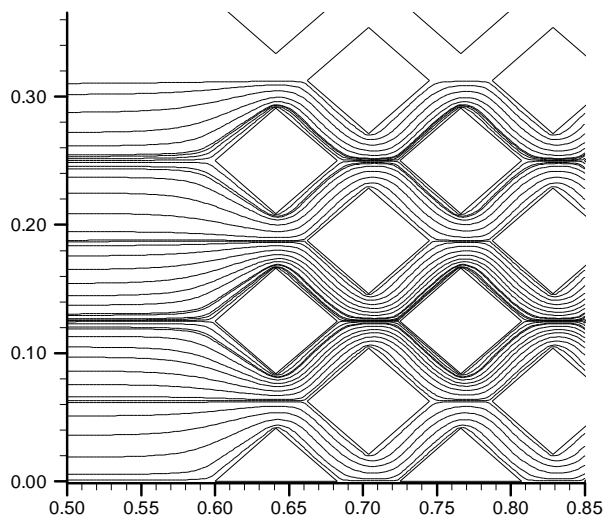


Figure 7 Isolines of stream function near first column of the catalyst needles ($Re=350$)

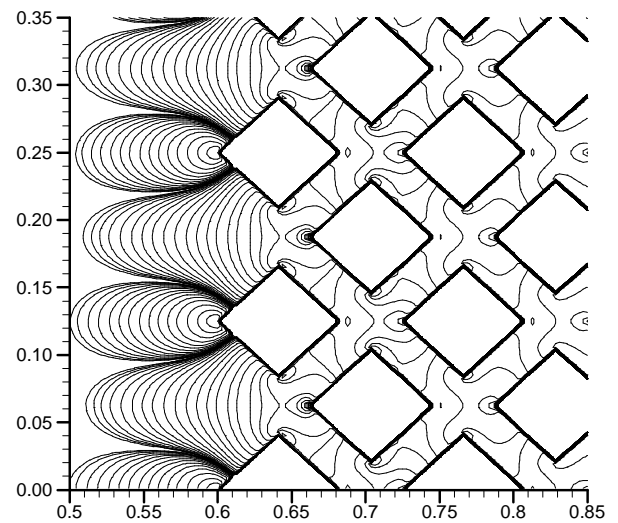


Figure 8 Isobars near first column of the catalyst needles ($Re=350$)

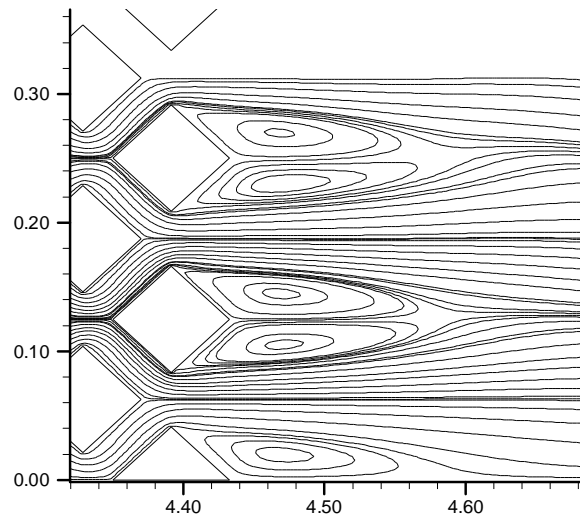


Figure 9 Vortex formation near last column of the catalyst needles ($Re=350$)

5. REFERENCES

- [1] D.B. Spalding, *The PHOENICS Beginner's Guide*. CHAM TR/100, CHAM Limited, London, 1990.
- [2] A.J. Chorin, A numerical method for solving incompressible viscous flow problems, *J. Comput. Phys.*, v. 2, pp.12–26, (1967).
- [3] W.R. Briley, Numerical method for predicting three-dimensional steady viscous flow in ducts, *J. Comp. Phys.*, v. 14, pp. 8–28, (1974).
- [4] U. Ghia, K.N. Ghia, C.T. Shin, High-Re Solutions for Incompressible Flow Using the Navier-Stokes Equations and a Multigrid Method, *J. Comp. Physics.*, v. 48, pp. 387–411, (1982).
- [5] I.E. Barton, The entrance effect of laminar flow over a backward-facing step geometry, *International Journal for Numerical Methods in Fluids*, v. 25, pp. 633–644, (1997).
- [6] D. Gartling A test problem for outflow boundary conditions-flow over a backward-facing step, *International Journal for Numerical Methods in Fluids*, v. 11, pp. 953–967(1990).
- [7] P.M. Gresho, D.K. Gartling, J.R. Torczynski, K.A. Cliffe, K.H. Winters, T.G. Garratt, A. Spence, J.W. Goodrich, Is a steady viscous incompressible two-dimensional flow over a backward-facing step at $Re=800$ stable?, *International Journal for Numerical Methods in Fluids*, v. 17, pp. 501–541, (1993).
- [8] J. Keskar, D.A. Lin, Computation of laminar backward-facing step flow at $Re=800$ with a spectral domain decomposition method, *International Journal for Numerical Methods in Fluids*, v. 29, pp. 411-427 (1999).